DEFORMATION RATE ESTIMATION ON CHANGING LANDSCAPES USING TEMPORARILY COHERENT POINT INSAR

Lei Zhang[(1)], Xiaoli Ding[(1)], Zhong Lu[(2)]

[(1)] The Hong Kong Polytechnic University, Hung Hom, KLN, Hong Kong, Email:{lslzhang;lsxlding}@polyu.edu.hk
[(2)] U.S. Geological Survey, Vancouver, Washington, USA, Email:lu@usgs.gov

ABSTRACT

In areas undergoing large scale constructional developments, such as cities in most of developing countries, there are abundant scatterers that are only partially coherent in some observation period. In fact these scatterers still carry high-quality phase information at least in a subset of interferograms allowing us to estimate the deformation rates from them. Here the partially coherent scatterers as well as the persistently coherent scatterers are termed as Temporarily Coherent Points (TCPs). In this paper we provide two approaches for TCP identification. One is based on offset deviations during image pair coregistration procedure and the other one is based on Ambiguity Mad Median Ratio (AMMR). Since the TCPs might keep coherent in a subset of interferograms, we propose two deformation parameter estimators that can either be performed only with coherent phases of TCPs or have the ability to suppress the effect of decorrelated phases and phase ambiguities that are considered as "outliers" when taking all interferograms as observations. We apply the techniques to map land surface deformation over Macau, China. The results from our TCPInSAR processing have been confirmed by ground measurements.

1. INTRUDUCTION

Multi-temporal InSAR (MT-InSAR) [1][2] is a useful tool for remote sensing of ground deformation. As the basic observations of current MT-InSAR techniques, persistently coherent scatterers can usually be densely identified from radar images over well-developed urban areas where the townscapes have evolved into a stable stage. With the dense coherent scatterers the current MT-InSAR techniques can be successfully applied. However there are many urban areas, especially in developing countries, which are undergoing rapid constructional development. Urbanization makes it difficult to identify abundant persistently coherent scatterers and thereby hampers us from achieving a better risk assessment over these areas. Over these changing landscapes, many scatterers cannot maintain consistently coherence during the whole observation time span even though they still carry high-quality phase signals at least in a certain period to allow for an estimate of land surface deformation [3][4].

The coherent points on changing landscapes can basically be classified into two types. One type is the persistently coherent scatterers (e.g., PS) and the other type is partially coherent points. Both of these points hereafter are referred to as Temporally Coherent Points (TCPs). In this paper we present a novel MT-InSAR analysis technique termed as TCPInSAR to identify the TCPs and retrieve ground deformation rates from these points. Regarding the identification of TCPs, besides the method shown in [5] which is an image pair based method, we also propose an image (amplitude) based method. The method is similar to the amplitude dispersion index [1], but based on the Ambiguity Mad Median Ratio (AMMR) that has the ability to isolate partially coherent points. To estimate deformation from these TCPs, we propose two parameter estimators. One is modified from [6] by involving a coherence index to remove interferograms where the point pair is not coherent simultaneously. The other estimator is especially designed for the TCPs selected by AMMR. Since AMMR dose not identify interferograms where the selected TCPs are coherent, when taking all interferograms as the phase times series for a given arc, some decorrelated phases might exist. Therefore we need to design a robust estimator that can suppress the effects of low-quality phases and the potential phase ambiguities at arcs to retrieve the deformation reliably. Here we select L_1 norm (also called least absolute deviations) estimator to meet our purpose, which has been used in [7] to improve the robustness of SBAS method. The basic observations of the proposed estimators are differential phases at arcs (point pairs) in multi-master interferograms with small spatial baselines, short temporal baselines, and small Doppler separations. One significant advantage of our estimators is that the deformation parameters can be estimated directly from the wrapped phases. In other words, there is no need of phase unwrapping. To evaluate the performance of the proposed TCPInSAR method, we choose the southern part of Macau as the test site. The area experienced rapid development from 2003 to 2010. Comparison with ground measurements has confirmed the validity of the results achieved through TCPInSAR method.

Proc. 'Fringe 2011 Workshop', Frascati, Italy,
19–23 September 2011 (ESA SP-697, January 2012)

2. TEMPORARILY COHERENT POINT INSAR

2.1. TCP identification

The identification of TCPs is the first core step in TCPInSAR processing. Two methods i.e., image pair based method and image based method, are introduced respectively in this section.

2.1.1 Image pair based method

The TCPs can primarily be identified based on the offset deviation in range and azimuth directions. The equation derived by Bamler and Eineder [8] indicates that standard errors of the estimated offsets from stronger scatterers is less sensitive to the window size and oversampling factor used in the image cross-correlation compared with those from distributed scatterers. Therefore it is possible to distinguish the strong scatterers from distributed scatterers by offset statistics. The detailed analysis and test of the method can be found in [5]. Here we propose an improved processing strategy which can significantly accelerate the TCP selection. Using the master image, we first identify points that can keep almost the same backscattering intensity when processed with fractional azimuth and range bandwidth as the TCP candidates. Second, TCP candidates are further evaluated by changing the size of patches and the oversampling factor in image cross-correlation. For the sake of simplicity, a fixed oversampling factor can be used. We can then obtain an offset vector ($\mathbf{OT_j}$) for a given TCP candidate (j) which includes the offsets ($ot_{ji}, i=1,\cdots,N$) estimated from N windows with changing sizes as shown in Eq.1. Points whose standard errors of offsets are less than a threshold are selected as TCPs. The threshold can be set as 0.1 considering the fact that when the precision of calculated offsets reaches 0.1 pixels or better, the coregistration error would be negligible [9].

$$\begin{aligned} &\mathbf{OT_j} = \begin{bmatrix} ot_{j1} & ot_{j2} & \cdots & ot_{jN} \end{bmatrix} \\ &std(\mathbf{OT_j}) < 0.1 \end{aligned} \tag{1}$$

The precise offsets at TCPs are actually the by-product of TCP selection, which can be used to resample the corresponding points in the slave images.

Since we identify the TCPs based on image pairs, we exactly know in which image pairs the points are coherent, which could work as an indicator to select interferograms for parameter estimation.

2.1.2 Image based method

Ferretti et al. proposed an amplitude dispersion index (σ_v) to identify the persistent scatterers (PS) according to the relationship between the amplitude stability and phase stability [1]. The index works well for radar targets having high phase stability over the whole observation period, however it can not identify scatterers behaving as PS only on a subset of images (i.e., partially coherent points). Here we propose a new index termed as Amplitude Mad Median Ratio (AMMR) that can identify the partially coherent points, which is defined as

$$\sigma_v \cong \frac{Mad_A}{Median_A} \tag{2}$$

Where $Median_A$ is the middle value of sorted intensity vector ($\mathbf{A}$) corresponding to a given pixel, and Mad_A is the median absolute deviation which is expressed as

$$Mad_A = Median(|\mathbf{A} - Median(\mathbf{A})|) \tag{3}$$

Simulation tests indicate that the AMMR can identify TCPs efficiently. We also found that if working with a criterion on minimum value of SLC intensities, the robustness of AMMR can be further improved. It should be noted that AMMR dose not indicate interferograms where the selected TCPs are coherent. Therefore when taking all interferograms as observations, we need to design a robust deformation parameter estimator that can suppress the effects of decorrelated phases and possible phase ambiguities.

2.2. TCP parameter estimator

In this section we provide two estimators that can retrieve deformation signals from wrapped interferometric phases without the need of phase wrapping. Since TCPs include the partially coherent points, we only estimate the height errors at TCPs and their linear LOS deformation rates.

2.2.1 Observation model

Phase differences at arcs constructed from two neighbouring TCP pixels are the basic observations of the deformation parameter estimators. Considering $J+1$ SAR images acquired in an ordered time sequence ($t_0 \quad t_1 \quad \cdots \quad t_J$) and I interferograms with short baselines. The phase difference ($\Delta\phi^i_{l,m,l',m'}$) at the arc constructed by TCP (l,m) and TCP (l',m') can be expressed as

$$\begin{aligned} \Delta\phi^i_{l,m,l',m'} &= \alpha^i_{l,m}\Delta h_{l,m,l',m'} + \beta_i \Delta V + w^i_{l,m,l',m'} \\ w^i_{l,m,l',m'} &= \Delta\phi^i_{atmo,l,m,l',m'} + \Delta\phi^i_{orbit,l,m,l',m'} + \Delta\phi^i_{dop,l,m,l',m'} \\ &\quad + \Delta\phi^i_{noise,l,m,l'm'} \end{aligned} \tag{4}$$

where $\Delta h_{l,m,l',m'}$ is the difference of the topography residuals at two TCPs and $\alpha^i_{l,m} = -\frac{4\pi}{\lambda}\frac{B^i_{\perp,l,m}}{r^i_{l,m}\sin\theta^i_{l,m}}$ is the

coefficient; $\Delta V = \left[\Delta v^1_{l,m,l',m'} \quad \Delta v^2_{l,m,l',m'} \quad \cdots \quad \Delta v^J_{l,m,l',m'} \right]^T$ is the differential deformation rate vector. When linear deformation is assumed, i.e., $\Delta v^1_{l,m,l',m'} = \Delta v^2_{l,m,l',m'} = \cdots = \Delta v^J_{l,m,l',m'} = \Delta v^{linear}_{l,m,l',m'}$, the vector has shrunk to $\Delta v^{linear}_{l,m,l',m'}$ and $\beta_i = -\frac{4\pi}{\lambda} \sum_{k=1}^{C_i - 1} (t_k - t_{k-1})$ is the corresponding coefficient; $w^i_{l,m,l',m'}$ includes differential phase related to atmospheric artifact ($\Delta\phi^i_{atmo,l,m,l',m'}$), orbital error ($\Delta\phi^i_{orbit,l,m,l',m'}$), Doppler centroid difference ($\Delta\phi^i_{dop,l,m,l',m'}$), and other noise ($\Delta\phi^i_{noise,l,m,l'm'}$). Because the differencing operation can significantly reduce the effects of spatially correlated atmospheric artifacts and baseline errors, $w^i_{l,m,l',m'}$ should be small and can be safely taken as a random variable with an expectation $E(w^i_{l,m,l',m'}) = 0$. The observation model for arcs without phase ambiguities can be expressed as

$$
\begin{aligned}
&\Delta\Phi = A \begin{bmatrix} \Delta h_{l,m,l',m'} \\ \Delta V \end{bmatrix} + W \\
&\Delta\Phi = \left[\Delta\phi^1_{l,m,l',m'} \quad \Delta\phi^2_{l,m,l',m'} \quad \cdots \quad \Delta\phi^I_{l,m,l',m'} \right] \\
&A = \left[\alpha \quad \beta \right] \\
&\alpha = \left[\alpha^1_{l,m} \quad \alpha^2_{l,m} \quad \cdots \quad \alpha^I_{l,m} \right]^T \\
&\beta = \left[\beta_1 \quad \beta_2 \quad \cdots \quad \beta_I \right]^T \\
&W = \left[w^1_{l,m,l',m'} \quad w^2_{l,m,l',m'} \quad \cdots \quad w^I_{l,m,l',m'} \right]
\end{aligned}
\qquad (5)
$$

where $\Delta\Phi$ is a vector containing phase differences between two adjacent pixels in a total of I interferograms. A is the design matrix including height-to-phase conversion factors and time combination matrix. W is a stochastic vector.

2.2.2 Least squares estimator with ambiguity detector

Before performing least squares on Eq. (5), we need to select interferograms for each arc to make sure the observations at the two TCPs are both the high quality differential phases (Fig.1).

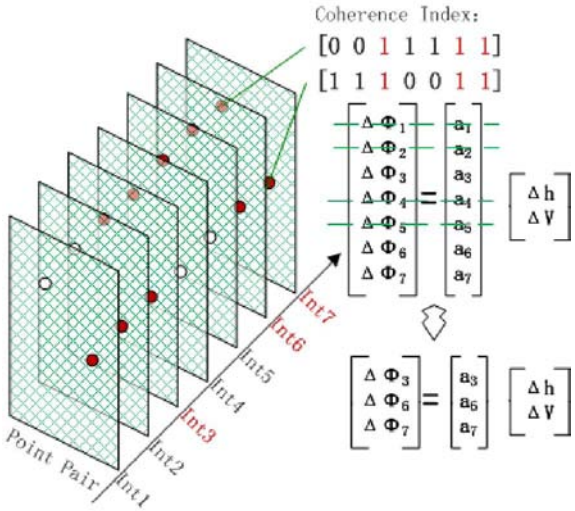

Figure 1. Illustration of interferogram selection for each arc before least squares.

With the remained observations, we can get the least squares solutions for each arc.

$$
\begin{aligned}
&\begin{bmatrix} \Delta\hat{h}_{l,m,l',m'} \\ \Delta\hat{V} \end{bmatrix} = \left(A^T P^{dd} A \right)^{-1} A^T P^{dd} \Delta\Phi \\
&\Delta\hat{\Phi} = A \left(A^T P^{dd} A \right)^{-1} A^T P^{dd} \Delta\Phi \\
&r = \Delta\Phi - A \left(A^T P^{dd} A \right)^{-1} A^T P^{dd} \Delta\Phi
\end{aligned}
\qquad (6)
$$

where the circumflex $\hat{}$ denotes estimated quantities; P^{dd} is the weight matrix which can be obtained by taking the inverse of the variance matrix of the double-difference phases and r is the least squares residuals. The corresponding covariance matrices of the estimated quantities are

$$
\begin{aligned}
&D\left\{ \begin{bmatrix} \Delta\hat{h}_{l,m,l',m'} \\ \Delta\hat{V} \end{bmatrix} \right\} = Q_{\hat{x}\hat{x}} = \left(A^T P^{dd} A \right)^{-1} \\
&D\left\{ \Delta\hat{\Phi} \right\} = Q_{\Delta\hat{\Phi}\Delta\hat{\Phi}} = A \left(A^T P^{dd} A \right)^{-1} A^T \\
&D\{r\} = Q_{rr} = Q_{dd} - A \left(A^T P^{dd} A \right)^{-1} A^T
\end{aligned}
\qquad (7)
$$

It should be noted that $\Delta\Phi$ might contain phase ambiguities at some arcs. The resolved parameters at these arcs are obviously wrong and we need to remove these arcs before getting the final parameters at TCPs. Comparison between least squares residuals of arc with and without phase ambiguities indicates that residuals can be used to isolate the arcs with ambiguities (Fig. 2). The details can be found in [6].

2.2.3 L_1 norm estimator

As mentioned before the TCPs selected by AMMR do not have a coherence index indicating interferograms

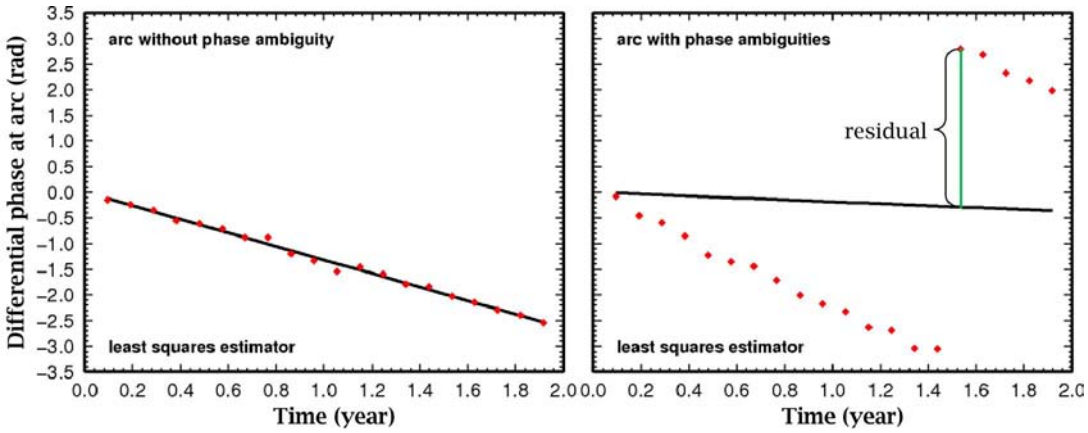

Figure 2. The least squares residuals at arcs with and without phase ambiguities

where they are coherent. Therefore we have to design a roust parameter estimator that can suppress the effects of low-quality phases and the potential phase ambiguities at arcs. L_1 norm estimator is no doubt a promising choice, which has been used in [7] for a robust SBAS. The performance of L_1 norm estimator on observations having decorrelated phases and phase ambiguities is shown in Fig. 3. L_1 norm estimator can be performed in many ways. Two typical ways are the iteratively reweighted least squares (IRLS) and linear programming. For a linear programming problem, L_1 norm of the observation model,

$$\text{minimize} \sum_i \left| \Delta\phi^i_{l,m,l',m'} - \sum_j A_{ij} \begin{bmatrix} \Delta h_{l,m,l',m'} \\ \Delta V \end{bmatrix} \right| \qquad (8)$$

can be rewritten as

$$\text{minimize} \sum_i f_i$$

$$\text{subject to} \quad f_i - \left| \Delta\phi^i_{l,m,l',m'} - \sum_j A_{ij} \begin{bmatrix} \Delta h_{l,m,l',m'} \\ \Delta V \end{bmatrix} \right| = 0 \qquad (9)$$

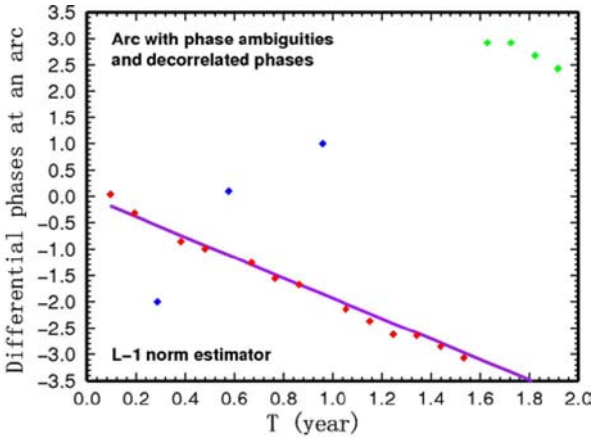

Figure 3. L_1 norm estimation on observations with decorrelated phases and phase ambiguities

which is equivalent to the following linear programming problem:

$$\text{minimize} \sum_i f_i$$

$$\text{subject to} \quad -f_i \le \Delta\phi^i_{l,m,l',m'} - \sum_j A_{ij} \begin{bmatrix} \Delta h_{l,m,l',m'} \\ \Delta V \end{bmatrix} \le f_i \qquad (10)$$

With a linear programming software package, Eq. (10) can be easily solved.

To evaluate the performance of the L_1 norm estimator, we test it on a set of differential phases at an arc (Fig.3). The result indicates that the L_1 norm estimator can precisely retrieve parameters from observations containing decorrelated phases and phase ambiguities.

2.2.4 TCP parameters

After obtaining the parameters (i.e., DEM errors and deformation rates) at arcs we can get the parameters at TCPs by spatial integration with respect to a given reference point, which can also be performed by least squares [6].

3. CASE STUDY

3.1. Test site and data

The southern part of Macau (Fig.4), which has experienced rapid development in the past ten years, is selected as our test site to evaluate the performance of the proposed TCPInSAR method.

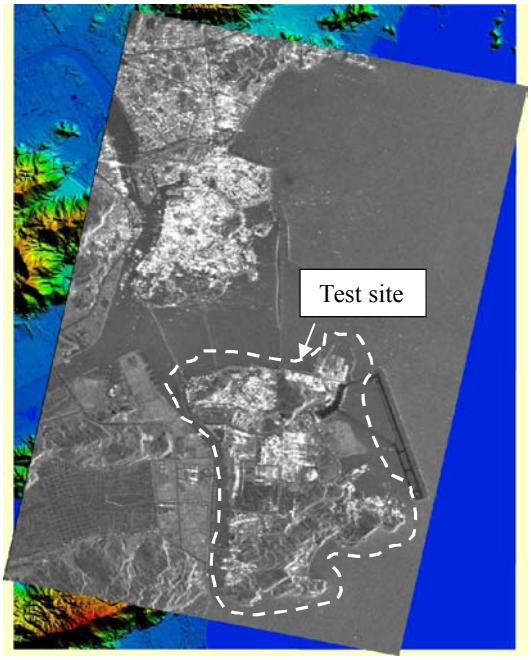

Figure 4. Test site

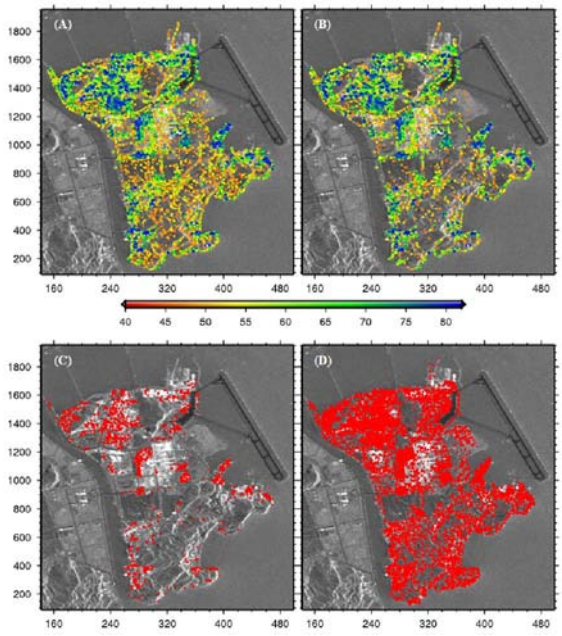

Figure 5. The location of TCPs selected by offset deviation (A), coherence (0.5) (B), amplitude dispersion index (0.6) (C) and AMMR (0.25) (D). The color bar indicates the appearing times of the TCPs in the interferograms

With a maximum spatial baseline of 150m, a maximum temporal baseline of 250 days and a maximum Doppler centroid difference of 300 Hz, we select 81 interferograms from 38 Envisat/ASAR images acquired in the period of 2003-2010.

3.2. Result

Offset deviation and AMMR are first employed to identify the TCPs shown in Fig. 5 together with the results from the coherence threshold and amplitude dispersion index. For TCPs selected by offset deviation, we perform the least squares estimation and ambiguity detector. The retrieved LOS linear deformation rate is shown in Fig.6 (A). For the TCPs selected by AMMR, we perform the L_1 norm estimator and the corresponding solution is shown in Fig.6 (B). Comparison with ground measurements provided by DSCC of Macau has confirmed the validity of the results achieved through TCPInSAR method.

4. CONLUSIONS

On changing landscapes, there are abundant scatterers that are not consistently coherent. However these scatterers still carry high quality phases in a subset of interferograms which can be used for the retrieval of deformation rates. In order to identify both the persistently coherent points and partially coherent points and reliably estimate the deformation rate at these points, we have proposed a new method named TCPInSAR consisting of two TCP identification thresholds and two robust deformation parameter estimators. The method has been applied to the southern part of Macau and the estimated deformation map has been validated by the ground measurements. Currently the TCPInSAR method is being applied on several other test sites with data acquired by different SAR sensors. Future work will focus on extensively validating the performance of TCPInSAR method.

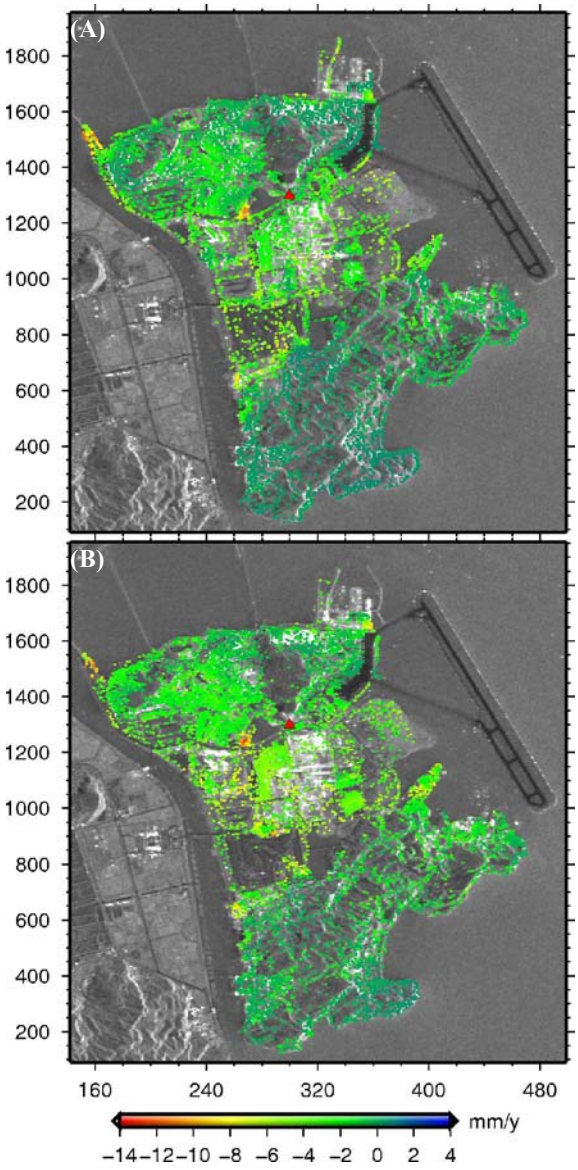

Figure 6. Deformation rate over Southern part of Macau estimated by least squares estimator with ambiguity detector (A) and L_1 norm estimator (B)

REFERENCES

[1] Ferretti, A., Prati, C., & Rocca, F. (2000). Nonlinear subsidence rate estimation using permanent scatterers in differential SAR interferometry. *IEEE Transactions on Geoscience and Remote Sensing, 38*, 2202-2212.

[2] Berardino, P., Fornaro, G., Lanari, R., & Sansosti, E. (2002). A new algorithm for surface deformation monitoring based on small baseline differential SAR interferograms. *IEEE Transactions on Geoscience and Remote Sensing, 40*, 2375-2383.

[3] Biggs, J., Wright, T., Lu, Z., & Parsons B. (2007). Multi-interferogram method for measuring interseismic deformation: Denali fault, Alaska. *Geophysical Journal International, 170, 1165-1179.*

[4] Biggs, J., Burgmann, R., Freymueller, J.T., Lu, Z., Parsons, B., Ryder, I., Schmalzle, G., & Wright, T. (2009). The postseismic response to the 2002 M 7.9 Denali Fault earthquake: constraints from InSAR 2003-2005. *Geophysical Journal International, 176*, 353-367.

[5] Zhang, L., Ding, X.L., & Lu, Z. (2011a). Ground settlement monitoring based on temporarily coherent points between two SAR acquisitions. *ISPRS Journal of Photogrammetry and Remote Sensing, 66*, 146-152.

[6] Zhang, L., Ding, X.L., & Lu, Z. (2011b). Modeling PSInSAR time series without phase unwrapping. *IEEE Transactions on Geoscience and Remote Sensing, 49*, 547-556.

[7] Lauknes, T. R., Zebker, H.A. and Larsen Y. (2011). InSAR deformation time series using an L_1-norm small- baseline approach. IEEE Transactions on Geoscience and Remote Sensing, 49, 536-546.

[8] Bamler, R., & Eineder, M. (2005). Accuracy of differential shift estimation by correlation and split-bandwidth interferometry for wideband and Delta-k SAR systems. *IEEE Geoscience and Remote Sensing Letters, 2*, 151-155.

[9] Hanssen, R. F. (2001). Radar interferometry: data interpretation and error analysis, Kluwer Academic Publishers.